

The role of Ni vacancies on the physical properties of $\text{CeNi}_x\text{Bi}_{2-y}$ single crystals

This content has been downloaded from IOPscience. Please scroll down to see the full text.

2015 J. Phys.: Conf. Ser. 592 012063

(<http://iopscience.iop.org/1742-6596/592/1/012063>)

View [the table of contents for this issue](#), or go to the [journal homepage](#) for more

Download details:

IP Address: 143.106.108.174

This content was downloaded on 04/05/2016 at 20:40

Please note that [terms and conditions apply](#).

The role of Ni vacancies on the physical properties of $\text{CeNi}_x\text{Bi}_{2-y}$ single crystals

P F S Rosa^{1,2}, C B R Jesus¹, C Adriano¹, Z Fisk², and P G Pagliuso¹

¹Instituto de Física “Gleb Wataghin”, UNICAMP, Campinas-SP, 13083-859, Brazil.

²University of California, Irvine, California 92697-4574, USA.

E-mail: pfsrosa@uci.edu

Abstract. The search for new superconductors (SC) represents an exciting field in condensed matter physics. Recently, $\text{CeNi}_{0.8}\text{Bi}_2$ has been reported as a new bulk SC ($T_c \sim 4.2$ K) in which Ni vacancies play an essential role for the emergence of superconductivity. Here we report experiments of magnetic susceptibility and heat capacity combined with energy dispersive X-ray spectroscopy analysis on $\text{CeNi}_x\text{Bi}_{2-y}$ ($x = 0.62, 0.70, 0.74, 0.78$) single crystals. Our data show a systematic enhancement of the antiferromagnetic transition temperature (T_N) with x , as well as the low temperature Ce^{3+} magnetic anisotropy. In particular, we find that the crystal-field ground state doublet becomes more isolated from the excited states as one approaches the Ni-rich end. As a consequence of such subtle crystal-field evolution, our analyses suggest that both the magnetic frustration and the hybridization between $\text{Ce}^{3+} 4f$ and conduction electrons are decreasing along the series. In addition, SC transitions are observed in both La and Ce members with no bulk signature, strongly indicating the presence of impurity SC phases.

1. Introduction

Cerium-based intermetallic compounds often present a rich and intricate interplay between the Ruderman-Kittel-Kasuya-Yosida (RKKY) magnetic interaction, the crystalline electrical field (CEF) effects, and the hybridization between $\text{Ce}^{3+} 4f$ and conduction electrons. As a result of this competition, a large variety of interesting physical properties may emerge, such as heavy-fermion (HF) behavior, quantum criticality, complex magnetic structures and unconventional superconductivity (SC) [1, 2, 3, 4]. In particular, the microscopic understanding of magnetic-mediated superconducting states in HF systems remains an open question that motivates further investigation. Interestingly, layered tetragonal structures host several Ce-based heavy fermion superconductors, such as $\text{Ce}M_2\text{Si}_2$ ($M = \text{Pd, Rh, Cu, Au}$), $\text{Ce}M_2\text{Ge}_2$ ($M = \text{Ni, Cu}$), $\text{Ce}M\text{In}_5$ ($M = \text{Co, Rh, Ir}$), Ce_2MIn_8 ($M = \text{Co, Rh, Pd}$), and CePt_2In_7 ($M = \text{Co, Rh, Ir, Pd}$) [5, 6, 7, 8, 9].

In this regard, the series of tetragonal intermetallic compounds CeTX_2 ($T = \text{transition metal, } X = \text{pnictogen}$) have recently attracted renewed attention due to the report of unconventional superconductivity at $T_c \sim 4$ K in polycrystalline samples of $\text{CeNi}_{0.8}\text{Bi}_2$ [10]. From macroscopic measurements, the presence of two types of carriers with distinct effective masses was inferred. In particular, the superconducting state, constituted by light carriers, has been claimed to coexist with the antiferromagnetic state at $T_N \sim 5$ K resultant from the interaction between $\text{Ce} 4f$ and heavy electrons. However, independent reports on single crystalline samples raised the question of whether superconductivity is an intrinsic property or a consequence of impurity phases, such as Ni-Bi binaries and Bi thin films [11, 12, 13].



Content from this work may be used under the terms of the [Creative Commons Attribution 3.0 licence](https://creativecommons.org/licenses/by/3.0/). Any further distribution of this work must maintain attribution to the author(s) and the title of the work, journal citation and DOI.

In order to shed new light on this controversy, here we systematically investigate the role of Ni vacancies on the physical properties of $\text{CeNi}_x\text{Bi}_{2-y}$ single crystals since Ni deficiency is reported to be crucial to the emergence of superconductivity. The studied compounds crystallize in the tetragonal ZrCuSi_2 -type structure (space group $P4/nmm$), with a stacking arrangement of CeBi-Ni-CeBi-Bi layers, and our results reveal that this structure presents intrinsic deficiency in the Ni site. Furthermore, we find that the antiferromagnetic ordering temperature (T_N) depends strongly on the Ni concentration and reaches 6 K at $x = 0.8$. Interestingly, both macroscopic measurements, namely magnetic susceptibility and specific heat, suggest an increase of the crystal-field parameter $|B_{20}|$, suggesting that the crystal-field ground state doublet becomes more isolated with x . Thus, our analyses suggest that both the magnetic frustration and the hybridization between $\text{Ce}^{3+} 4f$ and conduction electrons are decreasing along the series. In addition, no bulk response has been observed in magnetic susceptibility and specific heat measurements, confirming the extrinsic role of the binary compound NiBi_3 ($T_c = 4.2$ K) and Bi thin films ($T_c = 2 - 5$ K, depending on the thickness of the film) in the emergence of SC.

2. Experimental details

Single crystals of CeNiBi_2 and LaNiBi_2 were grown from Bi-flux with starting composition $\text{Ce:Ni:Bi}=1:x_{\text{nominal}}:8$. The mixture was placed in an alumina crucible and sealed in a quartz tube under vacuum. The sealed tube was heated up to 1050°C for 4 h and then cooled down at 6°C/h . The excess of Bi flux was removed at 800°C by centrifugation in order to avoid low temperature secondary phases. The single crystals with dimensions $\sim 5 \times 5 \times 0.5 \text{ mm}^3$ were grinded and their crystal structure was checked by X-ray powder diffraction experiments using $\text{Cu } K\alpha$ radiation at room temperature. Several single crystals from different batches were also submitted to elemental analysis using a commercial Energy Dispersive Spectroscopy (EDS) microprobe coupled to a FEG SEM microscope. From the EDS analysis, we have extracted the actual x_{Ni} concentration used throughout the text. The precision of the analysis was calculated by σ/\sqrt{N} , where σ is the standard deviation of the measurements, and N is the number of points analysed. Magnetization measurements were performed using a commercial superconducting quantum interference device (SQUID). Specific heat data were collected in a commercial Physical Properties Measurement System (PPMS) using a small mass calorimeter that employs a quasi-adiabatic thermal relaxation technique. The in-plane electrical resistivity data were also obtained in the PPMS system using a four-contact configuration.

3. Results and Discussion

Figure 1 displays the measured Ni concentration by EDS vs. the nominal concentration used in the growth. Interestingly, the data cannot be fitted to a straight line. In turn, the slope $dx_{\text{EDS}}/dx_{\text{nominal}}$ decreases as a function of Ni concentration and the x_{EDS} value tends to saturate around 0.8. This effect is likely due to two factors: (i) the decrease of Ni solubility in the melt since the Ni:Bi ratio increases; and (ii) the enhanced probability of formation of competing binary phases, such as NiBi and NiBi_3 . In fact, it has been recently verified that one can obtain the stoichiometric compound in $T = \text{Cu}$ sample, for which there are no obvious competing phases [14]. In addition, we find that the Bi occupancy remains constant for all the studied samples in the series. Nevertheless, it is worth noting that its value, $2 - y = 1.7$, is consistently less than 2. Although only cleaved samples were used in our measurements, we attribute this deficiency to the high air-sensitivity of the samples, which likely induces the formation of thin layers of Bi oxide on the surface.

We now turn our attention to the physical properties of the $\text{CeNi}_x\text{Bi}_{2-y}$ series. In order to better illustrate the underlying evolution along the series, we present the data of four representative Ni concentrations ($x_{\text{EDS}} = 0.62, 0.7, 0.74, 0.78$). Fig. 2 presents the temperature dependence of the magnetic susceptibility, $\chi(T)$, for an applied magnetic field $H = 1 \text{ kOe}$ parallel

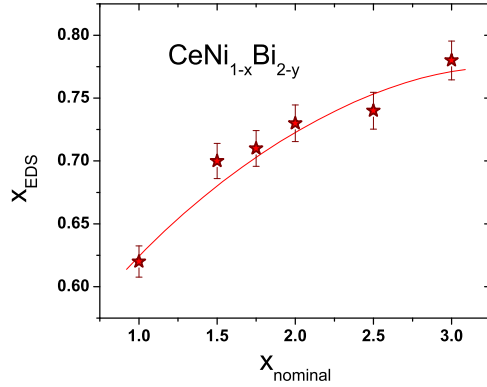


Figure 1. Measured Ni concentration vs nominal Ni concentration for the $\text{CeNi}_x\text{Bi}_{2-y}$ series.

(χ_{\parallel}) and perpendicular (χ_{\perp}) to the c -axis. The insets show the temperature dependence of the zero-field cooling (ZFC) and field cooling (FC) magnetic susceptibilities when a magnetic field of $H = 20$ Oe is applied parallel θ_{\parallel} to the c -axis. Firstly, we note that the diamagnetic response due to the superconducting phase is present in the ZFC curves, which are dominated by shielding effects, but is absent in the FC curves, which in turn are ruled by the Meissner effect. We note that, although pinning effects could influence the FC curves, they are not expected to be large in the studied compounds. Furthermore, even the shielding response shown in the ZFC curves does not exceed $\sim 10\%$ of the SC volume fraction expected for a bulk superconductor. Remarkably, the sample with the concentration claimed previously to be responsible for superconductivity, namely $x = 0.78$, does not induce any diamagnetic response in either ZFC or FC curves (Fig. 2d). In addition, it is noteworthy that the SC transition remains unchanged along the series at $T_c = 4.2$ K. All the above strongly indicates that the observed diamagnetic response is due to a non-bulk superconducting signal from the extrinsic binary superconductor NiBi_3 , which present the same T_c .

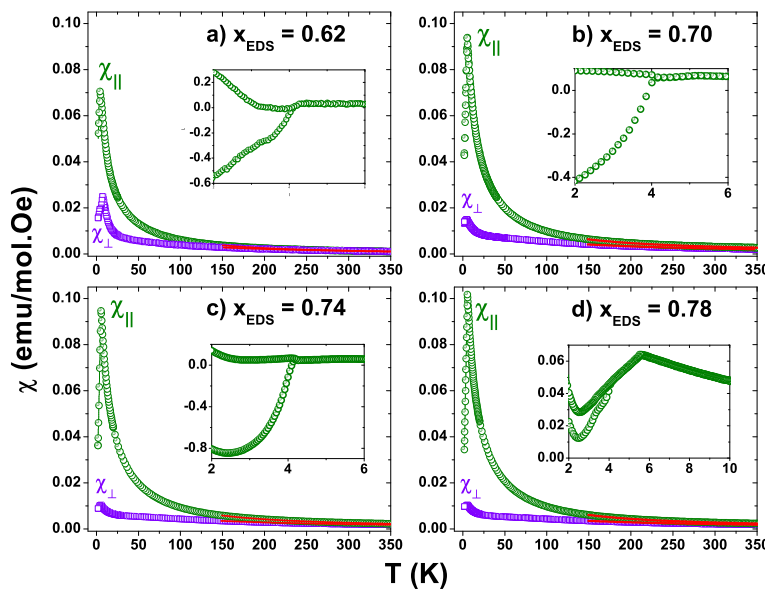


Figure 2. Temperature dependence of the magnetic susceptibility in the $\text{CeNi}_x\text{Bi}_{2-y}$ series measured with a magnetic field of $H = 1$ kOe applied (a) parallel θ_{\parallel} (open circles), and (b) perpendicular θ_{\perp} (open rectangles) to the c -axis. The red solid lines represent Curie-Weiss fits for $T > 150$ K. The inset show the diamagnetic signal obtained with an applied magnetic field of $H = 20$ Oe parallel to the c -axis.

At high temperatures ($T > 150$ K), $\chi(T)$ can be well fitted by a Curie-Weiss (CW) law plus a T -independent Pauli term, $\chi(T) = \chi_0 + C/(T - \theta_{CW})$ (solid lines). For all studied samples,

we obtain an effective moment of $\mu_{eff} \approx 2.6(1)\mu_B$ in both directions, in agreement with the theoretical value of $\mu_{eff} \approx 2.54\mu_B$ for Ce^{3+} free ions. On the other hand, the θ values are drastically anisotropic and vary systematically along the series, as shown in Fig. 3 and Table I. In a molecular field approximation, such anisotropy indicates the presence of two effective exchange interactions with opposite signs between the Ce^{3+} moments. Interestingly, it has been recently observed in $CeCuBi_2$ that the macroscopic properties could be well fit by a mean field model with tetragonal CEF only in the presence of anisotropic sign-changing RKKY interactions [14]. Thus, anisotropic exchange parameters appear to be an intrinsic characteristic in this series of compounds. In fact, recent inelastic neutron scattering (INS) measurements on $CeNi_{0.8}Bi_2$ also suggested the presence of anisotropic magnetic interactions [15].

Despite the AFM ground state displayed by $CeNi_xBi_{2-y}$ at low fields, the presence of ferromagnetic (FM) fluctuations along the c-axis becomes evident in the spin-flop transition of the $M(H)$ data presented in Figure 4. We find a clear transition from an antiferromagnetic to a ferromagnetic (FM) phase at the critical field $H_c = 46$ kOe when $H||c$ -axis whereas a linear behavior is observed when the field is applied perpendicular to the c-axis for fields up to $H = 70$ kOe. Interestingly, the value of H_c increases with increasing x , as shown in Table I. In addition, from Fig. 4 one can also extract the magnetic moment recovered at $H = 7$ T, m_0 . Analogously, we find that m_0 also increases with Ni-concentration. This evolution of both m_0 and H_c values are the first indication of an enhancement of localization of the $Ce^{3+} 4f$ electrons and a decrease of magnetic frustration along the series. Our subsequent analyses and experiments will help us to confirm this scenario.

Table 1. Extracted experimental parameters of the $CeNi_xBi_{2-y}$ series.

x_{EDS}	T_N (K)	$\theta_{ }$ (K)	θ_{\perp} (K)	θ_{poly} (K)	$\frac{\chi_{\perp}}{\chi_{ }}$	H_c (T)	m_0 (μ_B/Ce)	Δ_{CEF} (K)
0.62	4.3	9.0	-72.0	-30	2.8	3.8	0.8	82
0.70	5.0	12.4	-80.1	-29	6.3	4.2	1.2	-
0.74	5.2	18.0	-84.8	-21	9.0	4.4	1.3	140
0.78	5.5	19.1	-93.7	-22	9.9	4.6	1.4	175

Remarkably, despite the above mentioned highly anisotropic θ values, the fits to the polycrystalline average of the magnetic susceptibility provide a roughly constant θ_{poly} value of ~ 25 K, as shown in Fig. 3. In the molecular field approximation, this result strongly indicates that the effective exchange parameter between Ce^{3+} ions remains the same at high temperatures although T_N is changing systematically along the series. Thus, another interaction must be driven the evolution of T_N . Since θ_{poly} is constant, one possible explanation would be the evolution of the low-temperature Ce^{3+} ($J = 5/2$) crystal field scheme of levels and wave-functions, which can affect the RKKY interactions, the Kondo effect, and the degree of localization of the crystal field ground state [16].

Regarding the possible CEF effects, the CEF Hamiltonian for the tetragonal point symmetry can be written as $H_{CEF} = B_2^0 O_2^0 + B_4^0 O_4^0 + B_4^4 O_4^4$, where B_i^n are the CEF parameters, and O_i^n are the Stevens equivalent operators obtained from the angular momentum operators [17]. By using the simplified high-temperature expansion of the magnetic susceptibility, the value of the B_2^0 parameter, which accounts for the tetragonal symmetry, is known to be correlated to the paramagnetic Curie-Weiss temperatures as $B_2^0 \propto (\theta_{\perp} - \theta_{||})$. Remarkably, the difference between the anisotropic θ values indeed increase systematically with x along the $CeNi_xBi_2$ series, suggesting that the magnitude of B_{20} is also increasing. Interestingly, similar crystal-field tuning

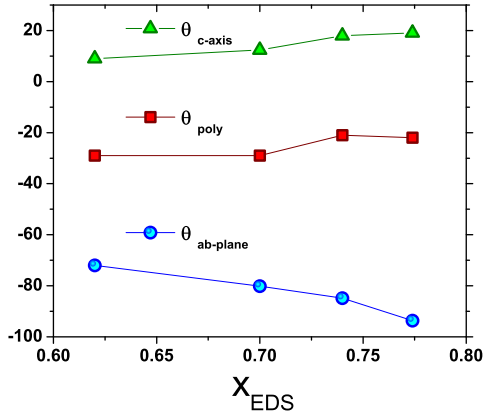


Figure 3. Evolution of the normalized paramagnetic Curie-Weiss temperatures for the studied $CeNi_xBi_2$ series.

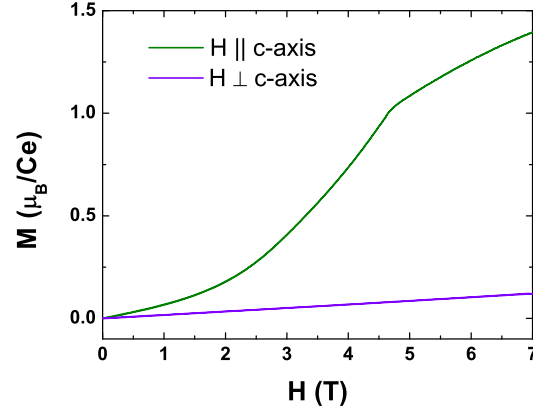


Figure 4. Magnetization as a function of the applied magnetic field at $T = 1.8$ K of the representative sample $CeNi_{0.78}Bi_2$.

of T_N has been observed in the tetragonal series R_mMIn_{3m+2} (R = rare-earth, M = Co, Rh, or Ir, $m = 1, 2$), which is known to host unconventional SC for $R = Ce$ [18, 19, 16]. In particular, for the $R = Tb, Nd$ tetragonal members, whose ordered moments also lie along the c -axis, T_N increases significantly when $|B_{20}|$ and/or the energy separation between the CEF ground state and the first excite state increases [18, 19, 16].

In addition, at low temperatures, $\chi(T)$ becomes anisotropic, consistent with an easy-axis along the c -direction, and presents a sharp drop at the onset of the antiferromagnetic (AFM) order. At T_N , the ratio $\chi_{||}/\chi_{\perp}$ is mainly determined by the tetragonal CEF and it also reflects the low- T Ce^{3+} single ion anisotropy. Interestingly, this ratio increases systematically with x along the series, also indicating that the main CEF parameter responsible for the tetragonal anisotropy, B_{20} , increases with x .

In order to confirm that the low-temperature doublet is becoming more isolated with x , we now turn our attention to the specific heat properties of the series. The total specific heat divided by temperature $C(T)/T$ as a function of the temperature for $CeNi_xBi_{2-y}$ (open symbols) and $LaNi_{0.7}Bi_2$ (solid line) is shown in Fig. 5a. The peak position of the $C(T)/T$ data occurs at $T_N = 4.3, 5.0, 5.2,$ and 5.5 K for $x = 0.62, 0.70, 0.74,$ and 0.78 , respectively, consistent with the AFM transition observed in the magnetization measurements. The inset shows $C(T)/T$ vs T^2 for the non-magnetic reference $LaNi_{0.7}Bi_2$, which can be well-fit by the classical expression $C = \gamma T + \beta T^3$ with $\gamma = 7.9$ mJ/mol.K² and $\beta = 2.4$ mJ/mol.K⁴. It is worth noting that no anomaly can be seen in C/T at low temperatures, although magnetic susceptibility measurements display the same SC behavior shown in Fig. 2 and transport measurements reveal zero-resistance superconducting transitions (not shown).

Finally, Fig. 5b presents the magnetic contribution to the specific heat, $C_{mag}(T)/T$, obtained by subtracting the data for the non-magnetic reference system. The solid lines in Fig. 5b are fits to the Schottky-type anomaly of two doublets separated by Δ_{CEF} . As shown in Table I, Δ_{CEF} in fact increases with x along the series, as one would expect from the increase of $|B_{20}|$ found in our magnetic susceptibility measurements. Therefore, both macroscopic properties strongly suggest that the CEF doublet ground state is becoming more isolated.

In addition, the magnetic entropy recovered can be obtained by integrating $C_{mag}(T)/T$. The inset of Fig. 5b shows the x dependence of the magnetic entropy recovered at T_N normalized by $R \ln 2$, which is the value expected for a doublet ground state in the CEF scheme of a Ce^{3+}

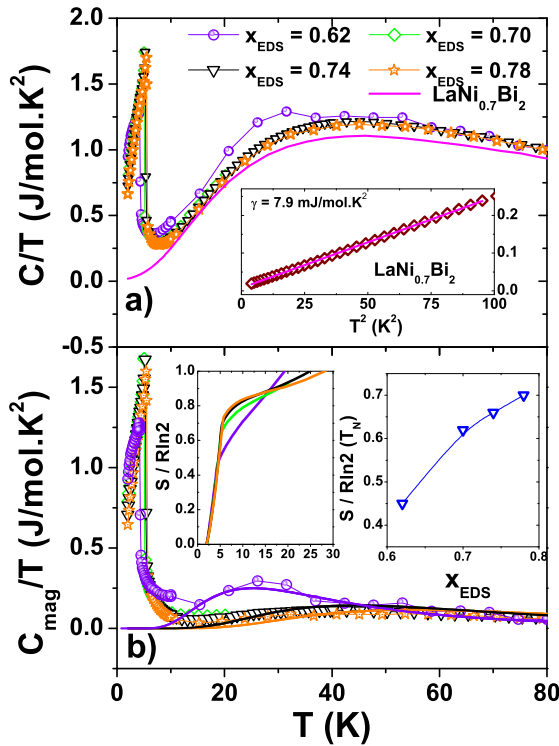


Figure 5. a) $C(T)/T$ as a function of temperature of CeNi_xBi_2 series (open symbols) and $\text{LaNi}_{0.7}\text{Bi}_2$ (solid line). The inset presents the low- T region of the specific heat of $\text{LaNi}_{0.7}\text{Bi}_2$. (b) $C_{\text{mag}}(T)/T$ as a function of temperature. The solid line represents a Schottky-type anomaly resulted from a two-level CEF scheme.

ion. Interestingly, the recovered entropy is found to increase from $\sim 45\%$ of $R\ln 2$ for $x = 0.62$ to $\sim 70\%$ of $R\ln 2$. The fact that the magnetic entropy recovered at T_N does not reach $R\ln 2$ has two possible causes. The first possibility is that this series of compounds display a slight Kondo-compensation of the Ce^{3+} CEF ground state magnetic moments. In fact, an estimate of the Sommerfeld coefficient γ by a simple entropy-balance construction, $[S(T_N - \epsilon) = S(T_N + \epsilon)]$, gives a moderately heavy fermion γ of $\sim 400 \text{ mJ.mol.K}^2$, consistent with a partial compensation. Therefore, one could speculate that $S(T_N)$ increases due to the systematic CEF induced decrease of the hybridization between the $\text{Ce}^{3+} 4f$ and the conduction electrons. Nevertheless, the above mentioned anisotropic magnetic susceptibility as well as the complex magnetic ordering indicate the possibility of magnetic frustration in this series of compounds. In fact, the ratio θ_{poly}/T_N goes from 7 to 4 with x . Thus, another possible scenario for the increase of the recovered magnetic entropy is the decrease of magnetic frustration along the series. In this case, the increase of the separation between the CEF ground state and the excited state would then favor the order along the [001] easy-axis at higher temperatures. We note that both scenarios are not mutually exclusive and most likely they occur simultaneously.

4. Conclusions

In summary, we have studied the evolution of the physical properties in $\text{CeNi}_x\text{Bi}_{2-y}$ single crystals as a function of Ni vacancies. Temperature dependent magnetic susceptibility and heat capacity experiments reveal a crystal-field induced increase of the antiferromagnetic ordering temperature with x . In particular, we find that the crystal-field ground state doublet becomes more isolated from the excited states as one approaches the Ni-rich end. As a consequence of such subtle CEF evolution, our analyses suggest the presence of both enhancement of localization of the $\text{Ce}^{3+} 4f$ electrons and the decrease of magnetic frustration along the series.

Acknowledgments

This work was supported by FAPESP-SP, AFOSR MURI, CNPq and FINEP-Brazil.

References

- [1] Fisk Z *et al.* 1995 *Proc. Natl. Acad. Sci. USA* **92** 6663
- [2] Pagliuso P G *et al.* 2001 *Phys. Rev. B* **64** 100503(R)
- [3] v Lohneysen H *et al.* 2007 *Rev. Mod. Phys.* **79** 1015
- [4] Petrovic C *et al.* 2003 *J. Mag. Magn. Mat.* **261** 210–221
- [5] Steglich F *et al.* 1979 *Phys. Rev. Lett.* **43** 1892
- [6] Grosche F M *et al.* 2001 *J. Phys.: Cond. Mat.* **13** 12
- [7] Jaccard D, Behnia K and Sierro J 1992 *Phys. Lett. A* **163** 475–480
- [8] Thompson J D and Fisk Z 2012 *J. Phys. Soc. Jpn.* **81** 011002
- [9] Bauer E D *et al.* 2010 *Phys. Rev. B* **81** 180507(R)
- [10] Mizoguchi H *et al.* 2011 *Phys. Rev. Lett.* **106** 057002
- [11] Thamizhavel A *et al.* 2003 *J. Phys. Soc. Jpn.* **72** 2632–2639
- [12] Lin X *et al.* 2013 *J. All. and Comp.* **554** 304–311
- [13] Jung M H *et al.* 2002 *Phys. Rev. B* **65** 132405
- [14] Adriano C *et al.* 2014 *arxiv:1407.2277*
- [15] Kim S W *et al.* 2014 *arxiv:1404.0129*
- [16] Pagliuso P G *et al.* 2006 *J. App. Phys.* **99** 08P703
- [17] Stevens K W H 1952 *Proc. Phys. Soc. A* **65** 209
- [18] Lora-Serrano R *et al.* 2006 *Phys. Rev. B* **74** 214404
- [19] Pagliuso P G *et al.* 2000 *Phys. Rev. B* **62** 12266